

Ultrasound: Medical Imaging and Beyond (An Invited Review)

Haim Azhari*

Dept. of Biomedical Eng. Technion IIT, Haifa 32000, Israel

Abstract: Medical applications of ultrasound were first investigated about seventy years ago. It has rapidly evolved since then, becoming an essential tool in medical imaging. Ultrasound ability to provide real time images with frame rates exceeding several hundred frames per second allows one to view rapid anatomical changes as well as to guide minimal invasive procedures. By combining Doppler techniques with anatomical images ultrasound provides real time quantitative flow information as well. It is portable, versatile, cost effective and considered sufficiently harmless to monitor pregnancy. Moreover, ultrasound has the unique capacity to offer therapeutic capabilities in addition to its outstanding imaging abilities. It can be used for physiotherapy, lithotripsy, and thermal ablation, and recent studies have demonstrated its usefulness in drug delivery, gene therapy and molecular imaging. The purpose of this article is to provide an introductory review of the field covering briefly topics from basic physics through current imaging methods to therapeutic applications.

Keywords: Ultrasound, imaging, waves, transducers, doppler, HIFU.

1. INTRODUCTION

Sound serves as our major means of communication. It is all around us. It helps us perceive our surroundings, from the whisper of the winds through the squeak of the birds to the sound of a thunder. It may affect our mood, e.g. through music, or reflect it, by laughter or cry. And as of the beginning of the twentieth century, it can also help us see the "invisible".

The first implementation of sound waves to "visualize" objects by mankind was probably in the military arena around the beginning of World War I (1914) with the introduction of the first underwater Sound Navigation and Ranging system (known as SONAR). In the years that followed (see [1] for an excellent historical review), many related technical developments, such as RADAR and metal flaw detectors, have led to the development of probably the first medical imaging system introduced by Dussik K.T. during World War II. This system attempted to map the brain using ultrasonic through-transmission imaging of the skull.

The field of medical ultrasound has substantially progressed since then, thanks to contributions made by numerous scientists and physicians. Among the more notable names are [1]: George Ludwig who began experiments with animal tissues using the A-mode (see following) in the late 1940s; John Julian Wild and John Reid who were the first to build a scanner that provided cross sectional ultrasonic images, which they coined as "echography" in the early 1950s; William Fry who pioneered the clinical use of high intensity ultrasound for ablating tissues in the 1950s; George Kossoff and co workers who have developed annular dynamic phased-arrays in 1974, which was a year later incorporated into a multi-transducer water-bath computerized scanner

called "UI-Octoson"; and James J Greenleaf who was the first to introduce an ultrasonic computed tomography (UCT) system in 1974 [2], which was mainly used for breast scanning.

The rapid developments in the fields of electronics, computers and material sciences have also projected progress onto the field of medical ultrasound. Current systems are: (i) very compact -there are portable palm sized scanners commercially available today; (ii) very rapid - combining phased array technology and advanced algorithms for image reconstruction; and (iii) highly computerized - enabling various types of real time rendering in 3D and 4D (i.e. space and time or function) and color coded flow mapping (see following).

In view of the facts that ultrasound is considered safe, radiation free, portable, compact, real time modality and cost effective, it is the most widely used cross-sectional imaging modality worldwide [47].

In this review article, the basics of medical ultrasonic imaging are introduced so as to present this fascinating field to the un-familiarized reader. In addition, some therapeutic ultrasound techniques are also briefly introduced.

2. BASICS OF ACOUSTIC WAVES

2.1. Definitions

Using simple terms, a wave is a phenomenon during which energy propagates from one location to another. In the case of acoustic (elastic) waves, the energy is mechanical and is stored in the elastic deformations of the material through which it travels and in the kinetic energy of its molecules. Importantly, while the molecules of the medium vibrate during the wave passage, mass is not transferred during the process. Consequently, it can be easily conceived that sound waves cannot travel through vacuum.

*Address correspondence to this author at the Dept. of Biomedical Eng. Technion IIT, Haifa 32000, Israel; Tel: 972-4-829-4145 (direct) or 4130 (office); Fax: 972-4-829-4599; E-mail: Haim@Bm.Technion.Ac.IL

The governing differential equation that describes this phenomenon is called the wave equation. In its most simplified form, for the case of a one-dimensional wave propagating within a homogeneous medium, it is given by:

$$\frac{\partial^2 U}{\partial x^2} = \frac{1}{C^2} \frac{\partial^2 U}{\partial t^2} \quad (1)$$

Where U is the wave function, x is the spatial coordinate (distance), t is the time and C is the wave velocity.

The solution for this equation, i.e. a wave function, has the general form of: $U(2\pi f \cdot t \mp K \cdot x)$, where f is the frequency, the parameter $K = \frac{2\pi}{\lambda}$ is called the "wave number",

and λ is the corresponding wave length. When the sign in the brackets is negative, i.e. a minus (-) sign, the wave propagates along the positive direction of the spatial coordinate. Conversely, a plus (+) sign implies that the wave propagates towards the negative direction.

There are several types of elastic waves defined according to the relation between the wave propagation direction and the particles displacement trajectories during the wave passage. The two most relevant types in the context of medical ultrasound are: (i) Longitudinal waves and (ii) Shear or transverse waves.

In the case of a longitudinal wave, the propagation direction of the wave coincides with the direction of the particle displacements within the medium see Fig. (1a). That is to say, if the wave travels along the horizontal direction, the vibrating molecules will also be displaced horizontally. It should be pointed out that since there is no mass transfer during the wave passage, the particles retain their equilibrium position by moving back and forth during the wave passage. Consequently, even during wave propagation towards the positive direction of the spatial coordinate, some material particles may be displaced towards the negative direction.

In the case of a transverse wave, the propagation direction of the wave is perpendicular to the direction of the particle displacements within the medium see Fig. (1b). Hence, if the wave travels along the horizontal direction, the vibrating molecules will be displaced vertically.

The speed of sound in each material depends on both its elastic properties and its density. Using very general terms, it could be stated that the higher the modulus of elasticity, i.e. the stiffer is the material, the higher is its corresponding speed of sound. Again, there is a distinction between longitudinal waves which rely on the material's ability to stretch or compress, and shear waves which depend on the material resistance to shear stresses, i.e. stresses which try to slide two adjacent material layers along opposite directions.

In soft tissues, the average speed of sound for longitudinal waves ranges from [3-8]: about 1450[m/sec] in fat to about 1590[m/sec] in the muscle. Typically, the average velocity is taken as 1520[m/sec]. It is worth noting that the skin has an exceptionally high speed of sound: 1730[m/sec]. In bones, the velocity of longitudinal waves is much higher and ranges around 3500-4100[m/sec]. The highest speed of

sound in the body is measured for longitudinal waves in the teeth enamel, and is about: 5500[m/sec].

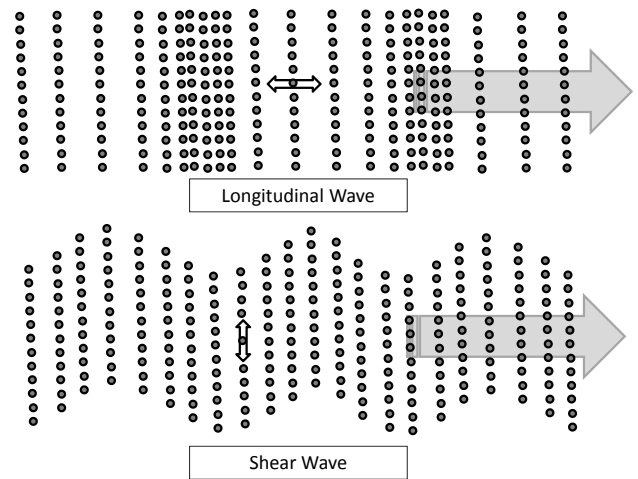


Fig. (1). Schematic depiction of the material's particles displacement under the two main ultrasonic wave types: (Top) When a longitudinal wave passes through the medium the particles vibrate back and forth parallel to the wave propagation direction. (Bottom) in a Shear wave the particles move along a perpendicular direction.

Shear waves, in comparison, have very low speed values in soft tissues. Common values (e.g. [9]), range around: 3-7[m/sec]. Furthermore, these values are frequency dependent [10]. Moreover, due to the rather fluidic nature of soft tissues and their limited ability to sustain shear stresses, shear wave decay is very rapid, particularly for higher frequencies. Thus, most applications which are based on shear wave measurements, e.g. MRI elastography [11], utilize low frequencies (smaller than a few hundred Hertz). Contrary to that, bones which have substantially higher shear modulus of elasticity have also much higher speed of sound for shear waves [12] (around 2800[m/sec]).

Another way to characterize waves is based on the wave front geometry see Fig. (2). Again, there are two main generic categories: (i) Planar waves and (ii) Spherical waves. Planar waves are generated when a large plate vibrates. The size of the plate has to be substantially larger (in fact infinite) than the wavelength in the medium in order to obtain a true planar wave. The vibrations can be either perpendicular to the surface of the transmitter – in this case longitudinal waves will be generated. Or, the vibrations can be parallel to the plate yielding shear waves which propagate into the medium. Either way, the wave front has a shape of a propagating plate. If attenuation in the medium is negligible, the amplitude of the waves is constant for all ranges.

Spherical waves are commonly generated when a point source vibrates or suddenly emits energy into the medium. The most familiar examples are explosions which typically generate spherical waves, or in the two dimensional case the circular waves that are generated when a pebble is thrown into a pond. In these cases, the wave fronts retain (if the medium is homogeneous) angular symmetry. A very important difference between this type of wave and a planar wave is

that even if the attenuation in the medium is negligible, the amplitude of the spherical wave will inversely diminish with the range.

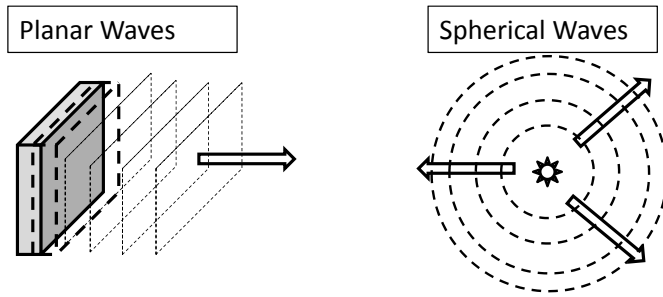


Fig. (2). Wave front propagation geometry for a planar wave (Left) and for a spherical wave (Right).

2.2. Transducers and Acoustic Fields

The most common method for generating ultrasonic waves is by using transducers made of piezoelectric materials. A piezoelectric material changes its geometry in response to an electric field applied to its surface. Consequently, the application of a time varying electrical field to a piezoelectric material will cause it to deform in a matching manner. The deformations will change the pressure at the transducer's surface and this will give rise to an acoustic wave which will travel into the medium. For example, by applying a sinusoidal voltage to a piezoelectric transducer, a sinusoidal continuous wave (CW) will be generated. On the other hand, by applying a sudden electric field to the surface, for a very short time (e.g. by discharging a loaded capacitor), yields a pulse wave. The central frequency and the frequency band of this pulse wave will be determined in this case by the transducer's properties and geometry. This quality of piezoelectric materials enables us to control the size, duration and profile of the transmitted waves very accurately. Generally speaking, CW is commonly used in therapeutic applications while pulses are commonly used for imaging.

Another great quality of a piezoelectric material is its ability to work as a receiver as well as a transmitter. This stems from the fact that when pressure is applied onto the piezoelectric material surface, voltage is generated. Consequently, by monitoring the voltage generated on the transducer's surface, we can actually monitor the pressures generated by impinging waves. Thus, a piezoelectric transducer can initially be activated as a transmitter by applying voltage to its surface for a short time. Then, by using fast switching and connecting an amplifier to the transducer, returning echoes impinging upon its surface can be registered in terms of voltage.

The acoustic field emitted from an ultrasonic transducer can be calculated using Huygens' Principle [13]. Using this principle, it is assumed that every point on the surface of the transducer emits spherical waves. The resulting field in the medium is the superposition of all interferences of these spherical waves.

In general, the two most used types of transducers are: (i) Mono-crystal disc transducers and (ii) Linear phased array transducers see Fig. (3).

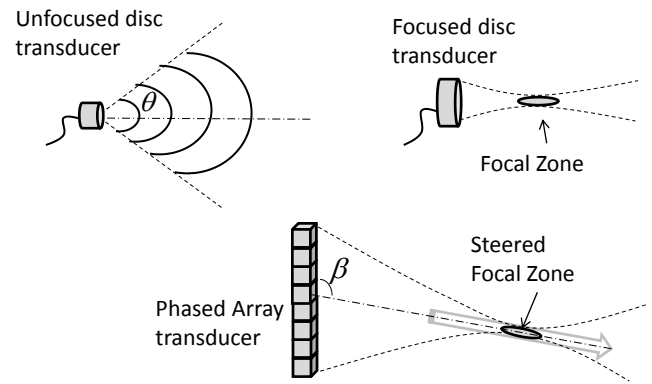


Fig. (3). Schematic depiction of the acoustic fields for a non-focused disc transducer (Top left), for a focused disc transducer (Top right) and for a linear phased array (Bottom). Note that with a phased array transducer the focal zone can be steered electronically.

The field emitted from an unfocused disc transducer diverges with distance. Basically, it can be divided into two zones: (i) The "near field" which is the field proximal to the surface, and where the intensity changes in a very abrupt manner many times; (ii) The "far field" where the intensity decays monotonically with the distance. The boundaries of the field's main lobe can be approximated by a conical geometry for which the head angle is given by,

$$\theta = \sin^{-1} \left(\frac{0.61\lambda}{a} \right), \quad (2)$$

Where λ is the wavelength in the medium and a is the radius of the disc transducer.

When using a focused transducer, the field converges until it reaches the focal zone, and then diverges again as shown schematically in Fig. (3). The focal zone has a typical cigar shape. The length of the focal zone ranges between 8-15 times its diameter depending on the transducer properties and the frequency used. The diameter of the focal zone D_{Focus} is approximately given by,

$$D_{Focus} \approx \lambda \cdot \left[\frac{F}{2a} \right], \quad (3)$$

Phased array transducers are made of many small elements placed proximal to each other in a circular or linear geometry. In most applications, a linear configuration is used (as shown schematically in Fig. 3). If the elements are sufficiently small, it can be assumed that each element transmits a spherical wave. The destructive interferences of these waves (stemming from opposite phases) will generate regions of acoustic "silence" in the medium while the constructive interferences will generate regions with high pressure amplitudes. The location of these zones can be controlled by controlling the transmission phase of each element. This process is called "beam-forming". Using beam-forming the shape and orientation of the acoustic beam can be altered. This enables us to steer the beam to different angles (β) and set its focal distance F electronically without physically moving the

array transducer. As shown schematically in Fig. (3), both tasks can be done simultaneously.

2.3. Reflection and Transmission

The most important material property associated with reflection and transmission is the "acoustic impedance". The acoustic impedance (Z) is defined as the multiplication of the volumetric density ρ by the speed of sound C ,

$$Z \triangleq \rho \cdot C \tag{4}$$

The acoustic impedance can be intuitively conceived as a virtual loaded wagon which the wave has to move in order to propagate.

A propagating acoustic wave will be partially or fully reflected when it encounters a discontinuity in the medium. The reflected waves are also called "echoes". The amplitude of a reflected echo normalized to the amplitude of the impinging wave is given for the most simple reflection model, i.e. a flat surface of uniform acoustic impedance (see Fig. (4) top) by,

$$R = \frac{Z_2 - Z_1}{Z_2 + Z_1} \tag{5}$$

Where Z_1 and Z_2 are the acoustic impedances of the first (where the wave arrive from) and second mediums, respectively. R is called the reflection coefficient and its value ranges between -1 to +1, $R = 0$ implies no reflection and $|R| = 1$ implies full reflection. The minus sign implies phase conversion. Thus, as schematically shown in Fig. (4)-Top, an incident wave of amplitude A_0 propagating from a medium of acoustic impedance Z_1 will be partially reflected when encountering a flat surface of a medium with acoustic impedance Z_2 . The amplitude of the echo is given by $R \cdot A_0$. The rest of the energy will continue its propagation into the second medium in the form of a through-transmitted wave.

In living tissues, the situation however, is much more complicated. There are many variations in the acoustic impedance per unit volume (see schematic depiction in Fig. (4)-Bottom). This gives rise to many small reflections and interferences of these waves. Consequently, an ultrasonic echo image has a typical speckle pattern, i.e. ultrasonic images seem to be comprised of numerous small bright dots on a black background. For example, an echo image of a liver is shown in Fig. (5). As can be noted, although the anatomy is uniform, the speckle texture governs the image. (The small black circular regions are blood vessels).

The typical values of the acoustic impedance for soft tissues is about 1.5×10^6 [kg / (sec. m^2)] while for bones its value is about 7.5×10^6 [Kg/(Sec. m^2)]. Metallic objects have even higher acoustic impedance. This implies that reflections between soft tissues are rather small (R is in the order of a few percent). Contrary to that, the reflections from bones are very strong. Hence, bones and metallic objects inserted into the body will be easily visualized. On the other hand, since most of the energy is reflected from the outer surface of the bone, it is almost impossible to image tissues located behind

it. That is a major obstacle that prevents, for example, brain imaging in the intact skull.

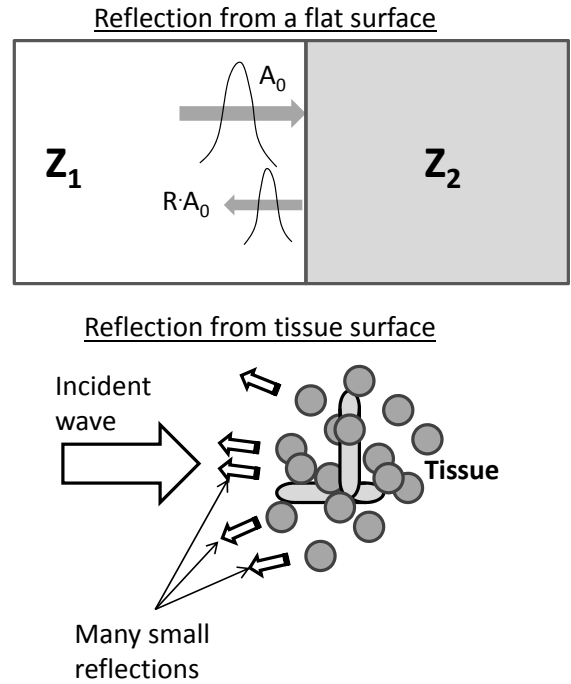


Fig. (4). (Top) A flat surface perpendicular to the ultrasonic beam will reflect an echo according to Eq. (5). The reflection pattern from a living tissue is much more complicated (Bottom).

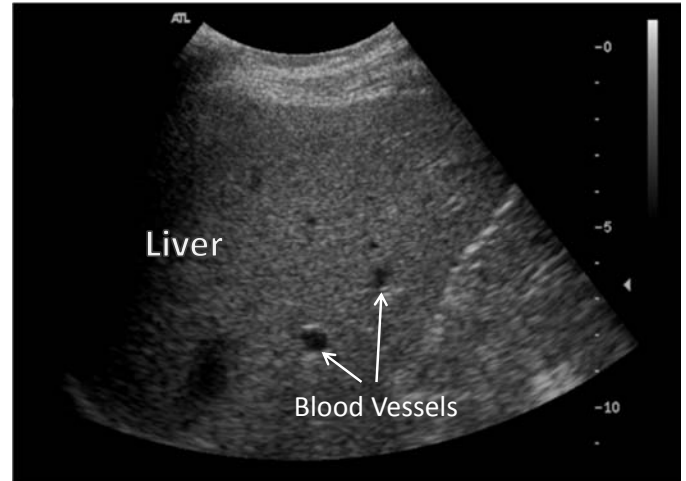


Fig. (5). A typical ultrasonic image obtained for a liver. Note the characteristic speckle texture.

Another problem stems from the fact that the acoustic impedance of air and gas is negligible. This implies that their reflection coefficient is about $|R| = 1$. As a result, it is impossible to image the lungs with currently available scanners. Moreover, as the heart is located between the ribs and the lungs, the acoustic imaging window for echocardiography is rather limited.

Finally, it should be pointed out that air can also be trapped between the surface of a transducer placed on the

body and the skin, particularly in hairy regions. Consequently, some of the transmitted acoustic energy will be reflected before reaching the skin, leading to poor image quality. As a remedy for that, water based gel is smeared prior to ultrasonic imaging in order to ensure adequate acoustic contact.

2.4. Attenuation

Another important phenomenon is attenuation. When transmitting a wave into a medium, the amplitude decays exponentially with the distance as shown schematically in Fig. (6). This applies to all wave types. The attenuation is commonly characterized by an attenuation coefficient α through the relation,

$$A(x) = A_0 \cdot e^{-\alpha x} \quad (6)$$

Where A_0 is the initial wave amplitude and $A(x)$ is the amplitude at distance x .

The attenuation can be intuitively conceived as a virtual barrier resisting the wave propagation. Hence, part of the wave's energy is absorbed with every distance that the wave propagates. The absorbed energy is commonly transformed into heat, giving rise to the local tissue temperature. Importantly, the attenuation coefficient depends on the wave's frequency. Its value increases as the frequency is increased. For the low megahertz range commonly used in medical imaging, this relation is almost linear, i.e. $\alpha(f) = \alpha_0 + \alpha_1 \times f$. Accordingly, waves with high frequencies have much lower penetration ability than low frequency waves. The typical attenuation coefficient for soft tissues is about 0.5db/cm/MHz, whereas for bones this value is much larger and ranges around 10-20db/cm/MHz. That is the second major obstacle that prevents ultrasonic imaging of the brain in the intact skull and other tissues located behind bones.

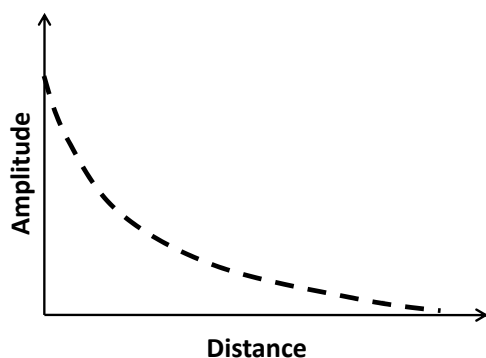


Fig. (6). Acoustic waves amplitude decays exponentially as a function of distance.

3. ULTRASONIC IMAGING

3.1. Definitions

In general, a medical image comprises two elements: (i) A spatial map- which provides information about the location of each tissue region relative to its surroundings; and (ii)

Contrast- which provides information about the imaged physical property of every specific tissue region manifesting graphically how distinct it is relative to its surrounding.

Current scanners commonly provide digital images formatted as a 2D or 3D matrix. Each element of the image matrix is called a "pixel" (or a "voxel" in the 3D case). The imaged physical property of each pixel is represented by a number assigned to it by the system. These numbers are in turn transformed into a scale of "gray-levels". That is to say, they are presented on the computer screen as lighted dots ranging from total black (assigned to the minimal value) to the brightest white (assigned to the maximal value). The intermediate levels are assigned various shades of gray.

Another important parameter related to imaging is resolution. The spatial resolution of an imaging system quantifies its ability to separate visually two adjacent targets located in close vicinity to each other. The spatial resolution depends mainly on the behavior of the acoustic field and the frequency. The higher the frequency, the potentially better is the spatial resolution. The resolution along the acoustic beam axis, i.e. the transmission direction, for frequencies in the range of several Mega Hertz is commonly in the order of a fraction of a millimeter. On the other hand the spatial resolution perpendicular to the acoustic beam, is in the order of a millimeter (depends on the location relative to the focal zone).

Temporal resolution quantifies the system's ability to detect two events proximal in time occurring at the same spatial location. In current ultrasonic imaging systems, the frame rate, which is the number of images depicted per second, exceeds several tens and even several hundred images per second. Recently, a new technology has been introduced that allows incredible frame rates reaching 5,000 images/sec [14]. With this technology, it is possible to image with unprecedented temporal resolution rapid changes in the tissue, such as its response to a HIFU impulse.

3.2. The A-Line

The basic building block for ultrasonic imaging is called the "A-line". An A-line is the echo train received after transmitting an ultrasonic pulse wave into the medium. A scan which depicts an A-line is called: "A-Mode" or "A-scan". The raw data of an A-line comprise all the radio-frequency (RF) signals detected by the transducer after transmitting a short pulse into the medium. The basic assumption is that all the detected signals are scattered waves, i.e. echoes, reflected along a straight "line-of-sight" (a one-dimensional configuration).

In order to understand how an A-line is formed, consider the following simple case: a short Gaussian pulse, i.e. a pulse with a Gaussian shaped spectral band, is transmitted towards a target which is composed of many parallel plates of different acoustic impedances located adjacent to each other and which surfaces are perpendicular to the acoustic beam see Fig. (7). At every point of discontinuity in the acoustic impedance value, (in this case at every boundary between two adjacent plates), an echo will be generated according to Eq.5 above. Ignoring reverberations and plotting these echoes as a function of time yields the basic RF A-line (Fig. (7) bottom). In order to relate time to range, it is assumed that

In order to relate time to range, it is assumed that the speed of sound is approximately constant with an average value of \bar{C} , and the distance is calculated using the following equation,

$$\text{Distance} = \frac{\Delta t \cdot \bar{C}}{2} \tag{7}$$

Where Δt is the time elapse between transmission and echo detection. The division by 2 is needed since the waves have to travel back and forth between the transducer and the point of reflection.

As depicted in Fig. (7), the amplitude of the echoes reduces with the range. This stems from attenuation and scatter processes. In order to compensate for this signal decay, it is common to employ time gain compensation (TGC). This is achieved by applying higher amplification for the more distal echoes.

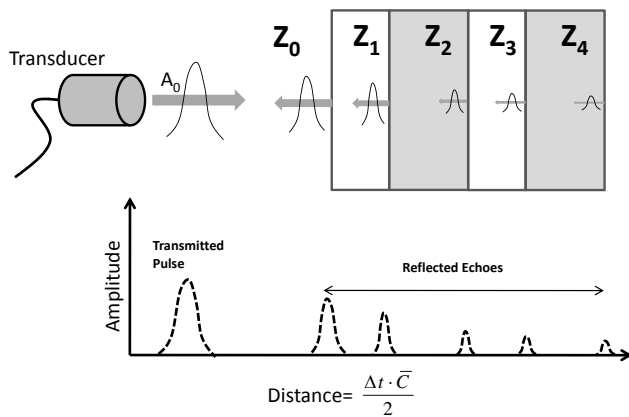


Fig. (7). An echo train is obtained when transmitting a wave towards a multilayered target.

The A-line from a real tissue on the other hand has a much more complicated texture, due to the numerous scattering points located within the tissue (as explained above). A typical A-line obtained from an ex-vivo muscle immersed in water is shown in Fig. (8). As can be noted, there are many reflections from within the tissue. The exponential decay stemming from attenuation is also clearly visible.

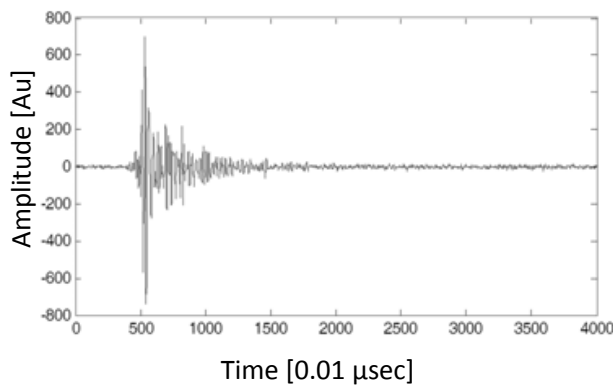


Fig. (8). A typical A-line obtained from an ex-vivo muscle specimen immersed in water.

3.3. M-Mode

The first two dimensional imaging technique following the formation of an A-line is called the "M-Mode", where the "M" stands for Motion. The idea is quite simple. Using a system which acquires many consecutive A-lines of a moving object, such as the heart walls, will display a gray level pattern which characterizes the motion of the studied organ. In the case of echocardiography, it will display a characteristic pattern of the heart's contraction (systole) and relaxation (diastole).

In order to build an M-Mode image, pulses are transmitted at a constant rate. This rate is titled: the pulse repetition frequency (PRF). Each time a pulse is transmitted, the corresponding A-line of a pre-defined range is registered. After applying some processing to the detected RF signal, it is transformed into a vector of gray levels. The transformation is composed of two steps: In the first step, the signal's envelope is extracted. This is done in order to eliminate the multiple ripples and amplitude variations associated with the RF signal and provides a smoother display. In the second step, the distance is binned into pixels and the average amplitude within each binned pixel is displayed as a gray level. This yields a row of pixels with varying gray levels corresponding to the echoes intensities and locations. The procedure is shown schematically in Fig. (9).

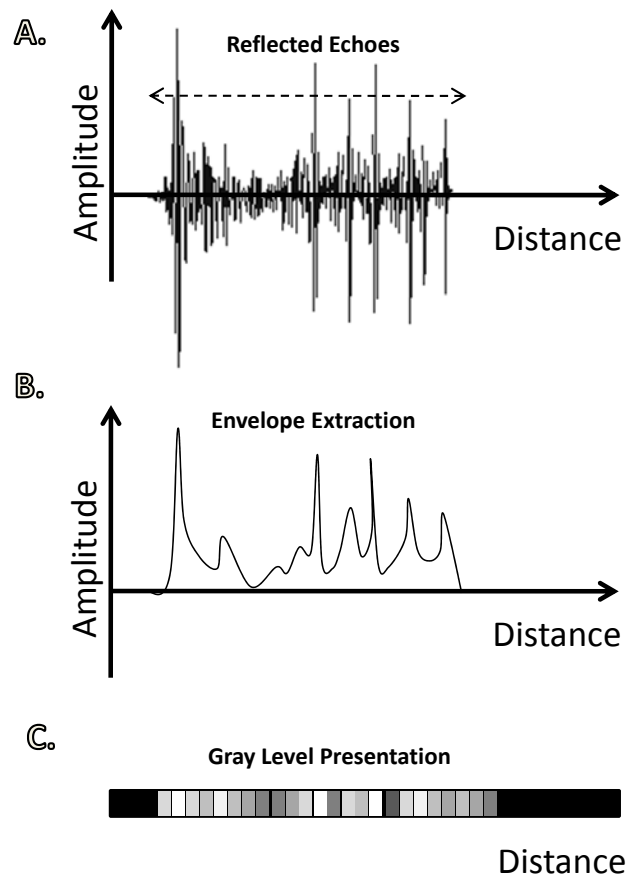


Fig. (9). The two basic steps applied to convert an echo-train signal (Top) into an image. In the first step, the signal's envelope is extracted (middle). Then the amplitude is converted into a vector of gray levels (Bottom).

The M-Mode image is generated by accumulating and displaying many gray level vectors side by side. Each row of pixels is repositioned as a column on the computer screen. The “oldest” vector is commonly displayed on the first column on the left of the display window and the “newest” vector is displayed on the last column which is commonly located on the right side of the display window. When a new vector is acquired, all columns are shifted to the left. The “oldest” column is omitted and the newest column is inserted on the right side of the picture. Using this format, the vertical direction represents the range from the transducer, and the horizontal direction represents time. (As recalled each column is acquired at time interval which is equal to $1/PRF$). A typical cardiac M-Mode image is depicted in Fig. (10).

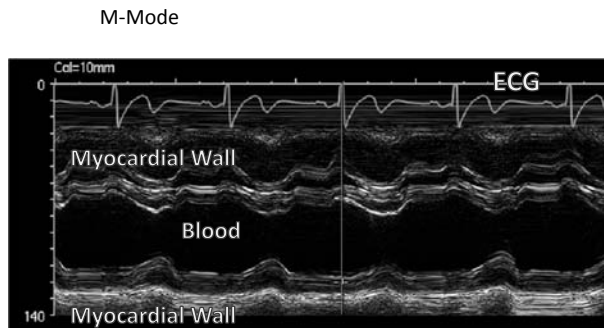


Fig. (10). A typical M-Mode image of the heart.

3.4. B-Scan

The most popular 2D imaging method is called “B-Scan”. This method is also based on the pulse-echo technique and is quite similar to radar or sonar imaging. The idea here is to scan a plane by transmitting short pulses along different directions and forming an image by tiling gray level echo vectors side by side. The procedure is almost identical to the one used for M-Mode, except for the fact that the acoustic beam is not stationary but is spatially steered to cover a plan.

In order to understand the technique, let us first assume that a Cartesian configuration is used see Fig. (11). The transducer, which is located at the top, transmits a series of parallel A-Lines. This can be done electronically using a phased array or mechanically by sliding a single element along the horizontal direction and transmitting a short pulse at predefined intervals. Using the procedure described above, the echo train relating to each pulse is transformed into a gray level vector. Naturally, the strongest echoes will be obtained from the boundaries separating two tissue layers which are perpendicular to the beam. Intermediate zones will produce the characteristic speckle pattern such as the one shown in Fig. (5). The reconstructed B-Scan image is formed by placing the echoes gray level vectors parallel to each other as shown schematically in Fig. (11). Once the scan has been completed, a new scan is initiated and each echo vector is replaced by a fresher one. The number of complete images obtained per second is called the frame rate. Modern systems can easily produce several tens of frames per second which may be considered “real-time imaging”. Hence, it is clearly understood why ultrasound is so popular in guiding minimal intervention procedures, e.g. needle insertions, etc.

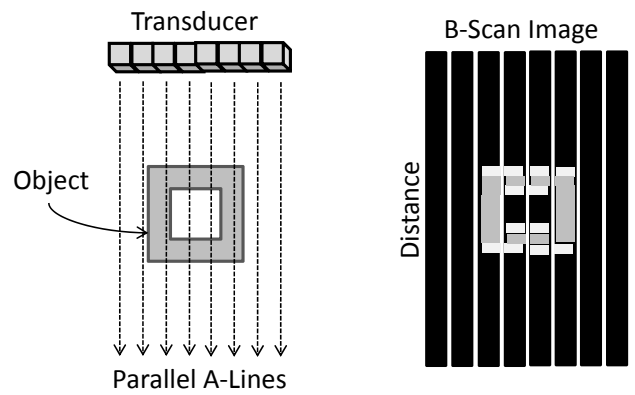


Fig. (11). Schematic depiction of the mapping layout utilized to generate a B-scan type image. (Left) The object is irradiated by many parallel A-lines. (Right) The corresponding gray level vectors are arranged accordingly to form the image.

Although Cartesian imaging is feasible, in many cases the size of the transducer is much smaller than the desired field of view (for example, in pregnancy monitoring or in echocardiography). In such cases, it is commonly more practical to scan the plane using a polar pattern similar to the pattern produced by the car’s wind shield wipers (or a pizza slice). This type of scan is called a sector scan. An exemplary echo-cardiographic image obtained by a sector scan depicting the heart’s left ventricle (LV) and its two valves is shown in Fig. (12).

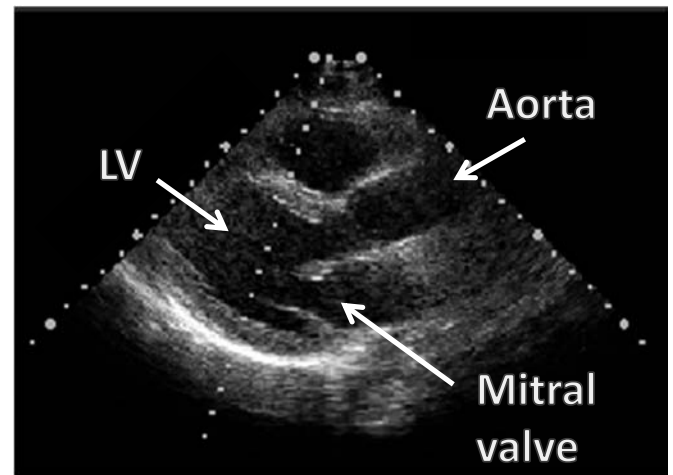


Fig. (12). A typical sector B-scan image obtained for a heart.

In recent years, 3D imaging has become popular. This type of imaging is merely an extension of the 2D B-Scan. Instead of scanning a sector of a plane, a conical or pyramidal volume is scanned. Again, the same principles described above are implemented. A short pulse is transmitted towards a predefined spatial direction and the resulting echoes are acquired and transformed into a gray level vector. However, from a technological point of view, 3D imaging poses several challenges. The amount of data that needs to be collected is huge and robust strategies for data collection and processing are needed.

3.5. Advanced Imaging Techniques

Although B-scan imaging dominates the clinics, there are several alternative techniques which can provide different type of information. The first method, which was suggested already in 1974 [2], is ultrasonic computed tomography (UCT). With this technique, through transmission is used instead of pulse-echo. A pair of transducers is positioned from both sides of the studied organ and waves transmitted from the first transducer pass through the object and are detected on the other side by the second one. The transducers are then rotated and through transmitted waves passing from a different angle are registered. By measuring the amplitude and/or the time of flight (i.e. the time it takes for the waves to travel from the first transducer to the other), both the attenuation coefficient and the speed of sound can be mapped using algorithms which are similar to those implemented in X-ray CT.

Unlike B-Scan, the information provided by UCT is much more quantitative and the geometry obtained does not assume that the speed of sound is constant (as done in B-Scan imaging). However, since a clear acoustic path is required in order to pass the waves (i.e. bones and gas will absorb or scatter them), this technique is limited almost exclusively to the breast. Nevertheless, since breast scanning is of utmost importance, UCT has been explored quite intensively [15-19] and several commercial systems have been suggested (e.g. [20]). Using UCT scanners 3D breast reconstructions can be obtained as well as projection images such as those produced by X-ray mammography. For example, an acoustic mammogram obtained at our lab with a UCT system is depicted in Fig. (13).

Acoustic Mammogram

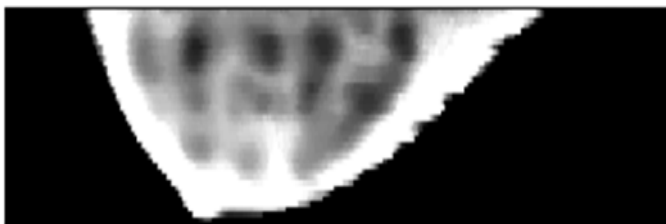


Fig. (13). A typical ultrasonic mammogram obtained at our laboratory using through transmission imaging.

Another imaging approach which has become an important research tool and has also recently become available for routine clinical use is called "Elastography". With this approach, the aim is map the tissue stiffness. The rationale for this approach stems from the fact that in many pathological conditions, the tissue of interest becomes stiffer than the surrounding healthy tissue. This stiffness abnormality can be detected by applying pressure on the tissue. That is why palpation is commonly used as a preliminary scanning examination in the clinic. However, manual palpation is neither quantitative nor reproducible. Ultrasonic elastography attempts to provide a more sensitive and systematic tool for performing the same task.

In order to understand the basic idea of elastography, consider an object which has a suspicious internal inclusion such as the one schematically shown in Fig. (14). If pressure is applied onto the object, it will deform and so will its internal structure. However, the internal deformations will differ according to the stiffness of the local tissue. The stiffer the tissue, the less it will deform. Thus, by using B-Scan imaging simultaneously with the squeezing process, the local deformations of the internal structures can be quantified and abnormally high stiffness regions can be detected. Although the idea seems simple, the processing algorithms are quite complicated. This stems from the fact that the internal stress field within the organ needs to be reliably estimated and that is not an easy task.

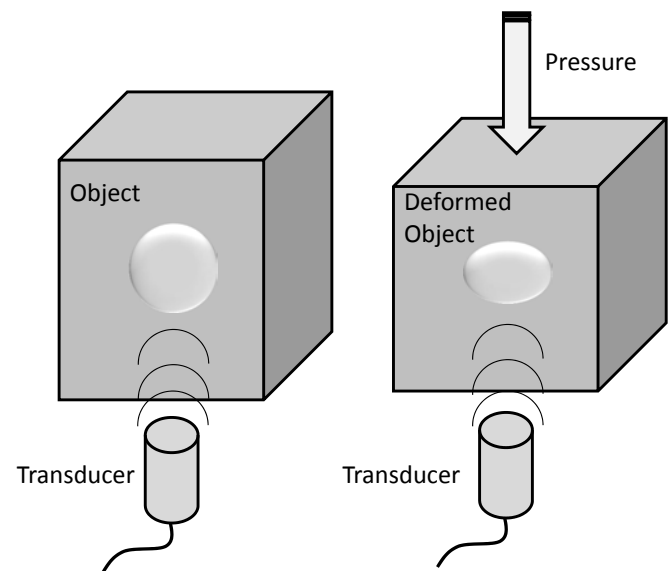


Fig. (14). The basic principle of ultrasonic elastography. A reference image is first obtained in an unloaded condition. Then images are acquired during the application of a pressure on the object. The corresponding deformations are used to display the tissue elasticity.

Many alternative approaches for elastographic imaging have been suggested. These include methods for vibrating the tissue in various modes and inducing shear waves within the tissue [21-25]. One elegant approach which provides non-invasive remote palpation has emerged in recent years. This method is called Acoustic Radiation Force Impulse (ARFI) imaging [26]. With this method, a short acoustic impulse is transmitted towards the target tissue. This is done by using high intensity focused ultrasound (HIFU). As a result, a substantial acoustic pressure is generated at the focal point along the beam propagation direction. This pressure pushes the target tissue and causes it to move and deform. By quantifying the tissue response to the ARFI, stiffer areas can be rapidly mapped and abnormalities detected in a non-invasive manner.

3.6. Ultrasonic Contrast Enhancing Materials

In order to augment the sensitivity of ultrasonic imaging and to map perfusion, the use of ultrasonic contrast enhancing (UCE) materials has been intensively explored. The basic concept of UCE was suggested by Gramiak and Shah already

in 1968 [27]. UCE is commonly made of very small gas bubbles coated by a polymetic shell or albumin. For example, one commercially available UCE which is called Definity™ (Bristol-Myers Squibb Medical Imaging, N. Billerica, MA, USA), comprises phospholipid-encapsulated perfluoropropane microbubbles. These microbubbles have diameters ranging from 1 μm to 10 μm . This allows them to pass the lungs and circulate in the blood stream for several minutes. Using B-scan imaging, the UCE microbubbles create strong echoes wherever they arrive. This stems from the fact that their acoustic impedance is almost negligible relative to that of the blood and tissues. Consequently, as may be deduced by substituting $Z_2 = 0$ into Eq.5, their reflection coefficient is equal to $R = 1$, i.e. total reflection. As a result, by imaging the tissue of interest prior to and post UCE injection, perfusion can be visualized.

Intravenous injection of UCE is used to improve image quality in pulse-echo and Doppler imaging [28]. B-scan imaging combined with UCE has also been proposed as a means of improving the differentiation of breast tumors [29,30] and also for kidney functional imaging [31].

3.7. The Doppler Effect

One of the unique and extremely useful features of ultrasonic imaging is its ability to non-invasively measure blood flow velocity [32]. This is done by exploiting the well known Doppler Effect. As recalled, when a wave of frequency f_0 impinges upon a moving target, it will be reflected with a different frequency f_1 . The discrepancy between the new frequency and the basic frequency Δf can be related to the target's velocity V via the following equation:

$$V = \frac{\Delta f \cdot C}{2f_0 \cos \theta} \quad (8)$$

Where C is the speed of sound in the medium and θ is the angle between the acoustic beam and the velocity direction of the target.

In the context of ultrasonic medical imaging, the Doppler Effect is commonly used to measure blood flow velocity in vessels and in the heart. The basic configuration is shown schematically in Fig. (15). A transducer is placed atop the skin proximal to the blood vessel of interest. In order to locate the blood vessel and determine the angle θ between the acoustic beam and the blood vessel axis, a 2D B-scan is usually performed prior to the Doppler acquisition. In some systems, the B-scan can be performed simultaneously with the Doppler acquisition and the two images are presented conveniently in two separate windows on the same screen. Once the blood vessel of interest has been located, the user can move a cursor (via computer mouse or a joystick) to the point of interest. Ultrasonic pulses are then transmitted towards this point. Reflections occur from the blood cells, since their acoustic impedance differs from the surrounding plasma. The detected echoes are then processed to determine the frequency shift Δf and the corresponding velocity is calculated according to Eq.8. The velocity temporal pattern is then depicted in a manner which resembles the M-Mode, with one important difference: the amplitude in this case

corresponds to velocity units. A typical example of a Doppler signal is shown in Fig. (16).

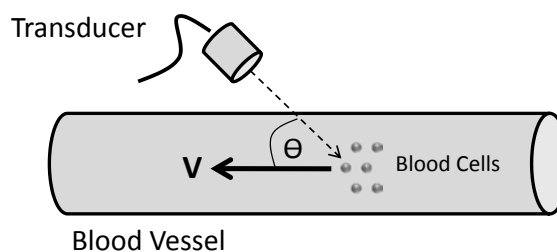


Fig. (15). The basic configuration utilized for measuring blood velocity via the Doppler Effect.

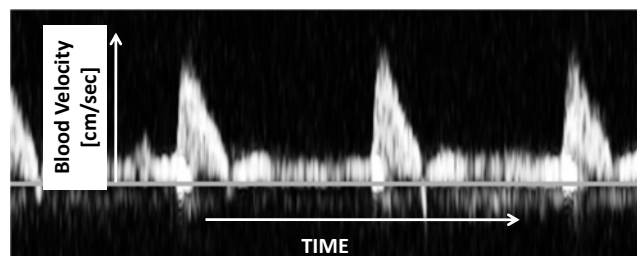


Fig. (16). A typical example of a Doppler signal displaying blood velocity as a function of time.

The above description explains how the velocity temporal pattern for a single region can be displayed. However, in many clinical applications, it is desired to map the velocity pattern within a large area. In such a case, the Doppler shift is calculated for every pixel within the region of interest. The corresponding velocity is then converted into pseudo-colors which are displayed as a graphic overlay atop the B-Scan image (which displays the anatomy). Commonly, the colors vary from red to blue, where flow towards the transducer is designated by red and flow away from the transducer is designated by blue (the colors can be switched by the user). This technique is referred to as color flow mapping (CFM). CFM is a very useful in cardiology as it can easily detect valve leakage (characterized by two colors and bidirectional flow) and stenosis (characterized by turbulence and high velocities).

In some applications, the flow direction is of lesser importance than the mere fact that there is flow in the region (e.g. in kidney imaging). In such cases, the direction sensitive red-blue CFM is replaced by a color-map which comprises shades of golden colors, where brighter colors correspond to higher flow rates. This mode is referred to as "Power-Doppler" imaging since it is obtained by integrating the corresponding Doppler power spectrum. The advantage of "Power-Doppler" is that (in principle) it should display similar color to vessels with equal flow regardless of the vessel's direction relative to the acoustic beam direction. Another advantage is that it is sensitive enough to display flow even in small blood vessels.

3.8. Molecular Imaging

Ultrasonic molecular imaging is an emerging research area which has advanced substantially in recent years. The

two main key components in this context are the use of very high frequency (40-200 MHz) imaging systems and UCE microbubbles [48]. Commercially available high frequency imaging systems operating at 40MHz, can be used to interrogate voxel size as small as: $40 \times 80 \times 80 \mu\text{m}^3$ (at the focal zone) [49]. This high spatial resolution can be useful for small animal and pre-clinical studies. The use of UCE materials in the form of microbubbles provides the needed marking component. As explained above, the microbubbles increase significantly the acoustic reflection of the volume in which they reside. Consequently, high concentration of microbubbles can be detected and be indicative to the physiological state of the tissue. The combination of high-frequency high-resolution ultrasound with the UCE microbubbles, therefore, offers a powerful research tool, which potential is currently investigated.

A promising approach to ultrasonic molecular imaging is the utilization of targeted microbubbles. Targeting is commonly achieved by attaching antibodies to the microbubbles shell. These antibodies serve as the ligand for the UCE material causing it to accumulate at the target tissue (e.g. tumors [50]). The localized enhanced concentration of the UCE material augments the acoustic reflectivity from the target making it detectable by ultrasonic imaging. A schematic description of this concept is depicted in Fig. (17). In this case a liposome serves as the microbubble shell. However, since liposomes disappear in the body within a short time if not protected. Poly-ethylene-glycol (PEG) coating is used to make it undetected by the macrophages. The antibodies are attached to the PEG shell in order to provide targeting capability. The gas within the liposome serves as the reflecting material (as explained above).

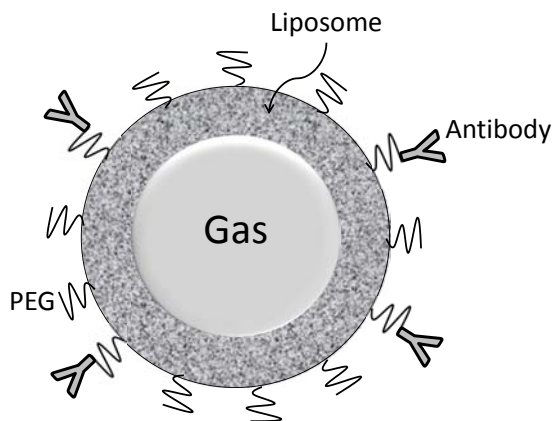


Fig. (17). A schematic description of the basic targeted molecular imaging element. A gas filled liposome coated by PEG is attached to antibodies. High concentration of such elements can be detected and displayed in a B-scan image.

4. THERAPEUTIC APPLICATIONS

Therapeutic ultrasound has been in use for many years [33]. Early applications were those for which tissue heating was the goal. Selective heating of selected regions within the body may induce vasorelaxation and accelerate the recovery process. This is utilized in order to promote healing in cases of tissue injury [34] and muscle soreness, such as may be

incurred during sport activities. The application of low intensity fields also appears to be able to stimulate physiological processes, such as tissue repair, without biologically significant temperature rises [33]. More recently, attention has been drawn to high intensity focused ultrasonic (HIFU) beams that may be used for thermal ablation of selected regions. Commonly guided by MRI, this offers a fully non-invasive surgery technology. Additional applications utilize ultrasonic induced cavitation bubbles (a non-thermal effect) for the destruction of tissues. In this review, the principles of physiotherapy and HIFU tissue ablation will be briefly presented.

4.1. Ultrasonic Physiotherapy

The basic mechanism which governs the ultrasonic physiotherapy process is the conversion of mechanical energy into heat. As explained above (see Eq.6), when an acoustic wave passes through the tissue its amplitude is reduced exponentially. This implies that its energy is also reduced. Although some of the energy is merely scattered, most of it is converted into heat. Hence, the gap between the ultrasonic energy entering a tissue element and the energy leaving it, serves as the energy source for the therapeutic process. This is shown schematically in Fig. (18).

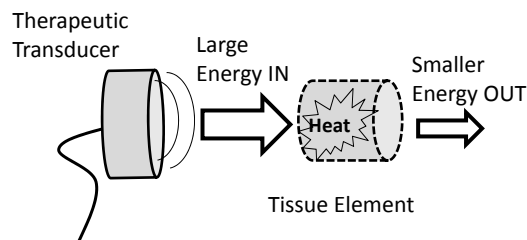


Fig. (18). The attenuation of the ultrasonic waves generates heat within the tissue. This heat can be utilized for therapeutic applications.

The intensities used in physiotherapy are smaller than $3[\text{Watts} / \text{cm}^2]$ for safety reasons. The temperature rise within the tissue depends on several factors. These include the transmitted intensity, the local attenuation coefficient (which as recalled depends on the wave's frequency), the specific heat and heat conductance coefficients of the tissue and the local heat removal rate by blood perfusion. Commonly, the temperature rise in ultrasonic physiotherapy is in the order of: 1-3°C.

4.2. High Intensity Focused Ultrasound (HIFU)

High intensity focused ultrasound (HIFU) is an emerging technology for non-invasive surgery. With the HIFU technique, a special ultrasound transducer (or an array of transducers) located near the treated organ is used as a virtual "knife" to destroy non-invasively a small volume of tissue within the body. The focused high acoustic energy induces a rapid and significant temperature rise at the focal point and causes local tissue ablation. (The temperature should exceed 57°C in order to induce complete cell death). Although suggested as early as the 1940s [37], HIFU has become very popular only in the past few years. This may be mainly at-

tributed to the integration of HIFU with modern imaging modalities. Image-guided HIFU surgery has been recently offered as a non-invasive alternative to conventional lumpectomy [38] in the breast [39-42] and in other organs [43-45].

The basic principles of HIFU surgery are schematically depicted in Fig. (19). The HIFU transducer, which is placed externally to the body, is acoustically coupled to the skin by water or gel. The focal zone, which has a typical cigar shape, is aimed towards the target tissue (e.g. a tumor) by using some image guidance modality (MRI or ultrasound). The wave intensity (energy per unit area) increases as the wave converges towards the focal zone. The intensity at the focal zone can reach several hundred watts (and even higher) per square centimeter. As a result, the temperature at this zone increases very rapidly. When the temperature exceeds 57°C, immediate cell death occurs. The HIFU transducer is then steered mechanically or electronically to ablate additional zones within the target tissue, until the complete destruction of the target is achieved.

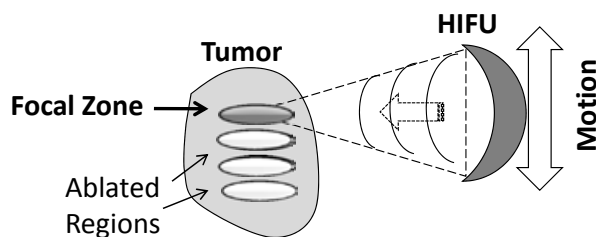


Fig. (19). The basic principles of HIFU surgery. The focal zone is aimed and moved within the target tissue in order to achieve complete thermal ablation.

It should be pointed, however, that although theoretically a temperature of 57°C is sufficient to kill the tissue in the focal zone, current systems aim to reach the temperature range of 70-80°C. This results in a larger killing zone due to heat dissipation. The phenomenon is demonstrated in Fig. (20) for ex-vivo turkey breast tissue exposed to HIFU of medium transmission intensity. As can be noted, while the classical narrow cigar shaped ablation (white tissue zone) occurs for a short exposure, the ablated zone for a long exposure is substantially larger.

Although there are still many technical issues that need to be resolved with this technology, HIFU is currently the only clinically practiced radiation free method for non-invasive surgery. In fact, as it is currently the most mature technology for non-invasive ablation of tumors, and following the title suggested by Kennedy *et al.* [46], it may well be considered the "surgical knife of the future".

4.3. Drug Delivery and Gene Therapy

Other applications of therapeutic ultrasound take advantage of its ability to open temporarily gateways in tissue membranes. The exposure of living cells to intensive ultrasonic radiation for a sufficiently long duration alters the cells membrane properties. The membrane can become highly permeable for a certain amount of time (in many cases the process is reversible). This permeability can be utilized for drug delivery and gene transfection.

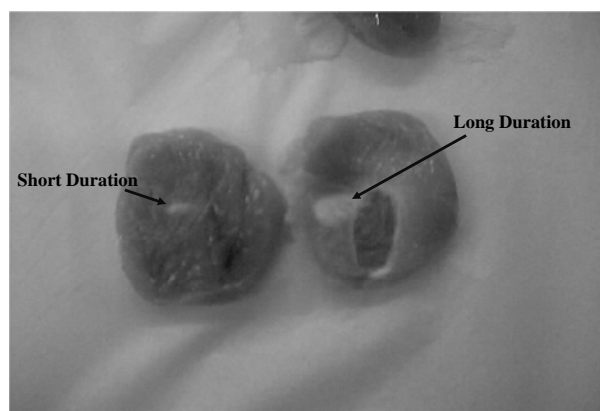


Fig. (20). The effect of heating duration on the size and shape of ablated region for an ex-vivo turkey breast tissue specimen.

One exemplary application is a device for trans-dermal drug delivery [35]. The device is based on an ultrasonic transducer which is attached to the skin and transmits waves with a frequency of 55 KHz. This induces the formation cavitation bubbles within the skin layer. The collapse of these bubbles lead to transdermal micro pathways. These micro pathways allow the transmission of fluids and chemical substances into and out of the body. The aim is to help diabetic patients.

An extensive research is also done in order to pass drugs through the blood-brain-barrier (BBB). Intensive ultrasound pulses transmitted to the brain under MRI guidance can disrupt the BBB reversibly and allow large drug molecules to reach the target (see for example [51]). Another approach utilizes thermosensitive liposomes for encapsulating drugs [52]. As explained in the section related to molecular imaging Fig. (17) these liposomes can be targeted by attachment to antibodies. When heated by an acoustic beam the liposomes release their payload at the target.

Gene therapy is yet another field which may benefit from ultrasound [36]. Using this approach, "repairing genes" commonly provided in a plasmid form need to be delivered into the nucleus of the treated cells without damaging the cells. The use of viral vectors for that purpose may bear the risk of mutations. Ultrasound on the other hand may provide a safer option and as was shown for example by [53] can achieve transfection using physiotherapy level intensities.

5. SUMMARY

In this review article, a glimpse into the world of medical ultrasound has been provided. The basic physical and the main technical principles of this modality in the context of imaging and therapy were introduced. As can be appreciated, ultrasound has currently many clinical applications and potentially new ones may be added in the near future.

ACKNOWLEDGEMENT

The author wishes to thank Dr. Diana Gaitini and Dr. Jonathan Lessick from the Rambam Health Care Campus, Haifa, Israel, for providing the clinical images.

CONFLICT OF INTEREST

The author(s) confirm that this article content has no conflicts of interest.

REFERENCES

- [1] Joseph Woo: *A short History of the development of Ultrasound in Obstetrics and Gynecology*. <http://www.ob-ultrasound.net/history1.html> (Accessed Sept. 12, 2011).
- [2] Greenleaf, J.F.; Johnson, S.A.; Lee, S.L.; Herman, G.T.; Wood, E.H. In: Algebraic Reconstruction of Spatial Distributions of Acoustic Absorption within Tissue from their Two-Dimensional Acoustic Projections. Acoustical Holography. Plenum Press. New York, 1974, 5, pp.966-972.
- [3] Duck, F.A. *Physical Properties of Tissue*, Academic Press, London, 1990.
- [4] Duck, F.A. In: *Propagation of Sound Through Tissue*. The safe use of ultrasound in medical diagnosis. Ter Haar, G.; Duck, F.A. Ed., *Br. Inst. Radiol.*, London, 2000, pp. 4-15.
- [5] Park, B.; Whittaker A. D.; Miller, R. K.; Hale, D. S. Predicting intramuscular fat in beef *longissimus* muscle from speed of sound. *J. Anim. Sci.*, 1994, 72, 109-116
- [6] Wells P.N.T. *Biomedical Ultrasonics*. Academic Press, New York, 1977.
- [7] Bamber, J.C.; Hill, C.R. Ultrasonic attenuation and propagation speed in mammalian tissues as a function of temperature. *Ultrasound Med. Biol.*, 1979, 5 (2), pp.149-157.
- [8] Kaye & Laby, Tables of Physical & Chemical Constants, National Physics Laboratory, UK, website, <http://www.kayelaby.npl.co.uk>. (Accessed Sept. 12, 2011).
- [9] Gluzman, T.; Azhari, H. "A method for characterization of tissue elastic properties combining ultrasonic computerized tomography with elastography". *J. Ultrasound Med.*, (JUM), 2010, 29, 387-398.
- [10] Catheline, S.; Wu, F.; Fink, M. A solution to diffraction biases in sonoelasticity: the acoustic impulse technique. *J. Acoust. Soc. Am.*, 1999, 105, 2941-2950.
- [11] Bishop, J.; Poole, G.; Leitch, M.; Plewes, D.B. Magnetic resonance imaging of shear wave propagation in excised tissue. *J. Magn. Reson. Imaging*, 1998, 8, 1257-1265.
- [12] Azhari, H. *Basics of Biomedical Ultrasound for Engineers*. John Wiley & Sons; Hoboken, New Jersey, 2010.
- [13] Ferwerda, H.A. Huygens' Principle 1690-1990: Theory and Applications, Proceedings of an International Symposium; Studies in Mathematical Physics. Blok, H.P.; Kuiken, H.K.; Ferweda, H.A. Editors, the Hague/Scheveningen, Holland, 1990, November, pp.19-22.
- [14] Bercoff, J.; Pernot, M.; Tanter, M.; Fink, M. Monitoring thermally-induced lesions with supersonic shear imaging. *Ultrason Imaging*, 2004, 26(2), 71-84.
- [15] Glover, G.H.; Sharp, J.C. Reconstruction of ultrasound propagation speed distributions in soft tissue: time-of-flight tomography. *IEEE Transactions on Sonics Ultrasonics*, 1977, SU-24, 4, 229-234.
- [16] Greenleaf, J.F.; Bahn, R.C. Clinical imaging with transmissive ultrasonic computerized tomography. *IEEE Transactions Biomed. Engr.*, 1981, BME-28:2:177-185.
- [17] Scherzinger, A.L.; Belgam, R.A.; Carson, P.L. Assessment of ultrasonic computed tomography in symptomatic breast patients by discriminant analysis. *Ultrasound Med. Biol.*, 1989, 15(1), 21-28.
- [18] Azhari, H.; Sazbon, D.; Volumetric imaging using spiral ultrasonic computed tomography. *Radiology*, 1999, 212(1), 270-275.
- [19] Glide, C.; Duric, N.; Littrup, P.; Novel approach to evaluating breast density utilizing ultrasound tomography. *Med. Phys.*, 2007, 34, 744-753.
- [20] TechniScan Medical Systems: URL: <http://www.techniscanmedicalsystems.com/index.php?p=Home>, (Accessed Sept. 14, 2011).
- [21] Ophir, J.; Alam, S.K.; Garra, B.S.; Kallel, F.; Konofagou, E.E.; Krouskop, T.; Merritt, C.R.B.; Riggetti, R.; Souchon, R.; Srinivasan, S.; Varghese, T.; Elastography: imaging the elastic properties of soft tissues with ultrasound. *J. Med. Ultrasonics.*, 2002, 29, 155-171.
- [22] Taylor, L.S.; Porter, B.C.; Rubens, D.J.; Parker, K.J. Three-dimensional sonoelastography: principles and practices. *Phys. Med. Biol.*, 2000, 45, pp.1477-1494.
- [22] Gao, L.; Parker K.J.; Lerner, R.M.; Levinson, S.F.; Imaging the elastic properties of tissue - a review. *Ultrasound Med Biol.*, 1996, 22(8), 959-977.
- [23] Greenleaf, J.F.; Fatemi, M.; Insana, M. Selected methods for imaging elastic properties of biological tissues. *Annu. Rev. Biomed. Eng.*, 2003, 5, 57-78.
- [24] Gennisson, J.L.; Catheline, S.; Chaffat, S.; Fink, M. Transient elastography in anisotropic medium: application to the measurement of slow and fast shear wave speeds in muscles. *J. Acoust. Soc. Am.*, 2003, 114(1), 536-541.
- [25] Catheline, S.; Thomas, J.L.; Wu, F.; Fink, M. Diffraction field of a low frequency vibrator in soft tissues using transient elastography. *IEEE Trans. Ultrason. Ferroelectr Freq Control*. 1999, 46(4), 1013-1019.
- [26] Palmeri, M. L.; Frinkley, K.D.; Zhai, L.; Gottfried, M.; Bentley, R. C.; Ludwig, K.; Nightingale, K. R. Acoustic radiation force impulse (ARFI) imaging of the gastrointestinal tract. *Ultrason Imaging*, 2005, 27(2), 75-88.
- [27] Gramiak R.; Shah P. Echocardiography of the aortic root. *Invest. Radiol.*, 1968, 3, 356-366.
- [28] Madjar, H. Contrast ultrasound in breast tumor characterization: present situation and future tracks. *Eur. J. Radiol.*, 2001, 11 (suppl 3), E41-E46.
- [29] Jung, E.M.; Jungius, K.P.; Rupp, N.; Gallegos, M.; Ritter, G.; Lenhart, M.; Clevert, D.A.; Kubale, R. Contrast enhanced harmonic ultrasound for differentiating breast tumors - First results. *Clin. Hemorheol. Micro.*, 2005, 33, 109-120.
- [30] Kettenbach, J.; Helbich, T.H.; Huber, S.; Zuna, I.; Dock, W. Computer-assisted quantitative assessment of power Doppler US: effects of microbubble contrast agent in the differentiation of breast tumors. *Eur. J. Radiol.*, 2005, 53, 238-244.
- [31] Verbeek, X.A.A.M.; Willigers, J.M.; Prinzen, F.W.; Peschar, M.; Ledoux, L.A.F.; Hoeks, A.P.G. High-resolution functional imaging with ultrasound contrast agents based on RF processing in an *in vivo* kidney experiment. *Ultrasound Med. Biol.*, 2001, 27, 223-233.
- [32] Jørgen, A. J. Estimation of Blood Velocities Using Ultrasound: A signal processing approach- Cambridge University Press, 1996.
- [33] Ter-Haar, G. Therapeutic ultrasound. *Eur. J. Ultrasound*, 1999, 9(1), 3-9.
- [34] Rantanen, J; Thorsson, O.; Wollmer, P.; Hurme, T.; Kalimo, H. Effects of therapeutic ultrasound on the regeneration of skeletal myofibers after experimental muscle injury. *Am. J. Sports Med.*, 1999, 27(1), 54-59.
- [35] Lavon, I.; Kost, J. Ultrasound and transdermal drug delivery. *Drug-Discov-Today*, 2004, 9(15), 670-676.
- [36] Duvshani-Eshet, M.; Baruch, L.; Kesselman, E.; Shimoni, E.; Machluf, M.; Therapeutic ultrasound mediated DNA to cell and nucleus: bioeffects revealed by confocal and atomic force microscopy. *Gene Ther.*, 2006, 13, 163-172.
- [37] Kremakau, F.W. Cancer therapy with ultrasound: A historical review. *J. Clin. Ultrasound*, 1979, 7, 287-300.
- [38] Randal, J. High intensity focused ultrasound makes its debut. *J. Natl. Cancer Institute*, 2002, 94(13), 962-864.
- [39] Hynynen, K.; Pomeroy, O.; Smith, D.; Huber, P.; McDannold, N.; Kettenbach, J.; Baum, J.; Singer, S.; Jolesz, F. MR imaging-guided focused ultrasound surgery of *fibroadenomas* in the breast: a feasibility study. *Radiology*, 2001, 219, 176-185.
- [40] Gianfelice, D.; Khiat, A.; Amara, M.; Belblidia, A.; Boulanger, Y.; MR imaging-guided focused ultrasound ablation of breast cancer: histopathologic assessment of efficacy - initial experience. *Radiology*, 2003, 227(3), 849-855.
- [41] Huber, P.E.; Jenne, J.W.; Rastert, R.; Simiantonakis, I.; Sinn, H.P.; Strittmatter, H.J.; von Fournier, D.; Wannemacher, M.F.; Debus, J. A new noninvasive approach in breast cancer therapy using magnetic resonance imaging-guided focused ultrasound surgery. *Cancer Res.*, 2001, 61(23), 8441-8447.
- [42] Gianfelice, D.; Abdesslem, K.; Boulanger, Y.; Amara, M.; Belblidia, A.; MR Imaging-Guided Focused Ultrasound Surgery (MRIgFUS) Of Breast Cancer: Correlation Between Dynamic Contrast-Enhanced MRI And Histopathologic Findings. *RSNA 2002*.
- [43] Tempany, C.M.C.; Stewart, E.A.; McDannold, N.; Quade, B.; Jolesz, F.; Hynynen, K. MRI guided focused ultrasound surgery (FUS) of uterine leiomyomas: a feasibility study. *Radiology*, 2003, 227, 897-905.

- [44] Wu, F.; Chen, W.Z.; Bai, J.; Zou, J.Z.; Wang, Z.L.; Zhu, H.; Wang, Z.B. Tumor vessel destruction resulting from high-intensity focused ultrasound in patients with solid malignancies. *Ultrasound Med. Biol.*, **2002**, 28(4),535-542.
- [45] Madersbacher, S.; Schatzl, G.; Djavan, B.; Stulnig, T.; Marberger, M.; Long-term outcome of transrectal high-intensity focused ultrasound therapy for benign prostatic hyperplasia. *Eur. Urology*, **2000**, 37, 687-694.
- [46] Kennedy, J.E.; Ter- Haar, G.R.; Cranston, D. High intensity focused ultrasound: Surgery of the future?". *Br. J. Radiol.*, **2003**, 76, 590-599.
- [47] Wells P.N.T. Physics and engineering: milestones in medicine. *Med. Eng. Phys.*, **2001**, 23,147-153.
- [48] Liang, H.D.; Blomley, M.J.K. The role of ultrasound in molecular imaging. *Br. J. Radiol.*, **2003**, 76 (2), 140-150.
- [49] Graham, K.C.; Wirtzfeld, L.A.; MacKenzie, L.T.; Postenka C.O.; Groom, A.C.; MacDonald, I.C.; Fenster, A.; Lacefield, J.C.; Chambers, A.F. Three-dimensional high-frequency ultrasound imaging for longitudinal evaluation of liver metastases in preclinical models. *Cancer Res.*, **2005**, 65(12), 5231-5237.
- [50] Lyshchik, A.; Fleischer, A.C.; Huamani, J.; Hallahan, D.E.; Brissova, M.; Gore J.C. Molecular imaging of vascular endothelial growth factor receptor 2 expression using targeted contrast-enhanced high-frequency ultrasonography. *J. Ultrasound Med.*, **2001**, 26, 1575-1586.
- [51] Kinoshita, M. Targeted drug delivery to the brain using focused ultrasound. *Topics Magnetic-Resonance-Imaging*, **2006**, 17(3), 209-215
- [52] Dromi, S.; Frenkel, V.; Luk, A.; Traughber, B.; Angstadt, M.; Bur, M.; Poff, J.; Xie, J.; Libutti, S.K.; Li, K.C.; Wood, B.J. Pulsed-high intensity focused ultrasound and low temperature-sensitive liposomes for enhanced targeted drug delivery and antitumor effect. *Clin. Cancer Res.*, **2007**, 13(9), 2722-2727.
- [53] Duvshani-Eshet, M.; Machluf, M. Therapeutic ultrasound optimization for gene delivery: a key factor achieving nuclear DNA localization. *J. Cont. Release*, **2005**, 108, 513-528.